THE JOURNAL OF BIOLOGICAL CHEMISTRY VOL. 287, NO. 27, pp. 22998–23009, June 29, 2012
Published in the U.S.A.

Lysyl Hydroxylase 3-mediated Glucosylation in Type I Collagen

MOLECULAR LOCI AND BIOLOGICAL SIGNIFICANCE[*S]

Received for publication, January 17, 2012, and in revised form, April 29, 2012 Published, JBC Papers in Press, May 9, 2012, DOI 10.1074/jbc.M112.343954

Marnisa Sricholpech[‡], Irina Perdivara[§], Megumi Yokoyama[‡], Hideaki Nagaoka[‡], Masahiko Terajima[‡], Kenneth B. Tomer[§], and Mitsuo Yamauchi[‡1]

From the [‡]North Carolina Oral Health Institute, School of Dentistry, University of North Carolina, Chapel Hill, North Carolina 27599 and the [§]Laboratory of Structural Biology, NIEHS, National Institutes of Health, Research Triangle Park, North Carolina 27709

Background: Type I collagen is the most abundant organic component in bone, providing form and stability.
Results: Lysyl hydroxylase 3-mediated glucosylation occurs at specific sites in collagen, including cross-linking sites, and suppression of this modification results in defective collagen and mineralization.
Conclusion: The data indicate the critical importance of this modification in bone physiology.
Significance: Alterations of this collagen modification may cause bone defects.

Recently, by employing the short hairpin RNA technology, we have generated MC3T3-E1 (MC)-derived clones stably suppressing lysyl hydroxylase 3 (LH3) (short hairpin (Sh) clones) and demonstrated the LH3 function as glucosyltransferase in type I collagen (Sricholpech, M., Perdivara, I., Nagaoka, H., Yokoyama, M., Tomer, K. B., and Yamauchi, M. (2011) Lysyl hydroxylase 3 glucosylates galactosylhydroxylysine residues in type I collagen in osteoblast culture. *J. Biol. Chem.* 286, 8846–8856). To further elucidate the biological significance of this modification, we characterized and compared type I collagen phenotypes produced by Sh clones and two control groups, MC and those transfected with empty vector. Mass spectrometric analysis identified five glycosylation sites in type I collagen (*i.e.* α1,2-87, α1,2-174, and α2-219. Of these, the predominant glycosylation site was α1-87, one of the major helical cross-linking sites. In Sh collagen, the abundance of glucosylgalactosylhydroxylysine was significantly decreased at all of the five sites with a concomitant increase in galactosylhydroxylysine at four of these sites. The collagen cross-links were significantly diminished in Sh clones, and, for the major cross-link, dihydroxylysinonorleucine (DHLNL), glucosylgalactosyl-DHLNL was diminished with a concomitant increase in galactosyl-DHLNL. When subjected to *in vitro* incubation, in Sh clones, the rate of decrease in DHLNL was lower, whereas the rate of increase in its maturational cross-link, pyridinoline, was comparable with controls. Furthermore, in Sh clones, the mean diameters of collagen fibrils were significantly larger, and the onset of mineralized nodule formation was delayed when compared with those of controls. These results indicate that the LH3-mediated glucosylation occurs at the specific molecular loci in the type I collagen molecule and plays critical roles in controlling collagen cross-linking, fibrillogenesis, and mineralization.

O-Linked glycosylation of hydroxylysine (Hyl)[2] residues has long been known to be a unique post-translational modification for collagens and proteins with collagenous sequences (1–3). This modification is catalyzed by two groups of collagen glycosyltransferases, hydroxylysine galactosyltransferase (EC 2.4.1.50) and galactosylhydroxylysine glucosyltransferase (EC 2.4.1.66), resulting in the formation of galactosylhydroxylysine (G-Hyl) and glucosylgalactosylhydroxylysine (GG-Hyl), respectively (4). It has been reported that the hydroxylysine galactosyltransferase activity is catalyzed by the multifunctional enzyme lysyl hydroxylase 3 (LH3) (5, 6) and the recently identified glycosyltransferase family 25 domains 1 and 2 (GLT25D1 and -D2) (7). The galactosylhydroxylysine glucosyltransferase activity, on the other hand, was found to be mainly catalyzed by LH3 (5, 8–12).

The pattern of collagen glycosylation varies depending on collagen types (1, 2), functional regions within the same tissue/same collagen type (13, 14), maturation (15–17), and pathological conditions (18–25). In bone, type I collagen is relatively less glycosylated (15, 26, 27); however, in bone/skeletal disorders, such as osteogenesis imperfecta (20, 28–30), postmenopausal osteoporosis (19, 23, 31, 32), osteosarcoma, osteofibrous dysplasia (21), and Kashin-Beck disease (33), altered collagen glycosylation occurs, and this has been implicated in mineralization defects. Due to the structure of the carbohydrates and the glycosylation sites, structural as well as biological functions have been proposed for collagen glycosylation (*i.e.* control of collagen fibrillogenesis (33–37), cross-linking (38–42), remodeling (33), collagen-cell interaction (43, 44), and induction of vessel-like structures (45)), all of which are important for the formation of functional fibrils for biomineralization. Despite all

* This work was supported, in whole or in part, by National Institutes of Health Grants R21 DE019569, DE020909, and AR060978 and the Intramural Research Program of National Institutes of Health, NIEHS, Project ES050171.

[S] This article contains supplemental Table 1 and Figs. 1 and 2.

[1] To whom correspondence should be addressed: CB#7454, NC Oral Health Institute, University of North Carolina, Chapel Hill, NC 27599. Tel.: 919-537-3217; Fax: 919-966-3683; E-mail: mitsuo_yamauchi@dentistry.unc.edu.

[2] The abbreviations used are: Hyl, hydroxylysine; MC, MC3T3-E1; EV, MC cell-derived clone stably transfected with empty vector; Sh, short hairpin (MC cell-derived clones stably suppressing LH3); G-, galactosyl-; GG-, glucosylgalactosyl-; deH-, dehydro-; DHLNL, dihydroxylysinonorleucine; HLNL, hydroxylysinonorleucine; HNL, hydroxynorleucine; LH3, lysyl hydroxylase 3; Pyr, pyridinoline; ESI, electrospray ionization; LOX, lysyl oxidase; ETD, electron transfer dissociation; BisTris, 2-[bis(2-hydroxyethyl)amino]-2-(hydroxymethyl)propane-1,3-diol.

of the findings regarding collagen glycosylation reported to date, the precise molecular loci, the extent/type of glycosylation, and their biological functions are still not clearly defined.

In our recent report (12), by employing the short hairpin (Sh) RNA technology, we have demonstrated that the major function of LH3 for type I collagen is to transfer glucose units to G-Hyl residues and that alteration in the level of glucosylation significantly affects the kinetics of collagen fibrillogenesis *in vitro*. In the present study, by using this system, we identified the LH3-mediated glucosylation sites in type I collagen and investigated the potential roles of this modification in type I collagen phenotypes by analyzing cross-linking pattern and maturation, fibrillogenesis, and matrix mineralization.

EXPERIMENTAL PROCEDURES

Cell Culture, Generation of Sh Clones, and Purification of Type I Collagen

The pSilencer2.1-U6/neo-Plod3 construct encoding the short hairpin sequence targeting *Plod3* was generated, and the MC3T3-E1 (MC) cell-derived clones stably suppressing *Plod3* (Sh clones) were obtained as described previously (12). MC cells and those transfected with the original pSilencer2.1-U6/neo plasmid (EV; encoding a hairpin siRNA sequence not found in any genome database) were used as controls. The phenotype of type I collagen synthesized by three Sh clones (Sh1-1, Sh1-2, and Sh1-3) and controls were further characterized in this study.

Identification of Glycosylated Hyl Residues by Mass Spectrometry

α Chain Separation and Proteolysis—Type I collagen was purified from MC, EV, and Sh clones as reported (12), and the α1 and α2 chains were separated by SDS-PAGE on 4–12% Bis-Tris precast gels (Invitrogen) for 1 h at 200 V, 100 mA, and 10 W. Following staining with Coomassie Simply Blue, the protein bands were excised and subjected to automated in-gel digestion with trypsin overnight at 37 °C, using a Progest robot digester (Genomic Solutions, Harbor, MI). The samples were lyophilized and stored at −80 °C until further use.

Mass Spectrometry—The collagen proteolytic mixtures were analyzed by LC-MS on a Waters-Micromass Q-Tof Premier hybrid tandem mass spectrometer equipped with a nanoAcquity UPLC system (Waters, Milford, MA). The lyophilized tryptic digests were reconstituted in 30–40 μl of 0.1% formic acid in deionized water. Analyses were performed on a 1.7-μm, 100 μm × 100-mm, BEH dC18 column (Waters, Milford, MA), using a flow rate of 300 nl/min. A C18 trapping column (180 μm × 20 mm) with a 5-μm particle size (Waters, Milford, MA) was positioned in-line of the analytical column and upstream of a micro-tee union used both as a vent for trapping and as a liquid junction. Trapping was performed for 3 min at a 5 μl/min flow rate, using the initial solvent composition. A 3-μl aliquot of the digest sample was injected onto the column. Peptides were eluted by using a linear gradient from 98% solvent A (0.1% formic acid in water (v/v)) and 2% solvent B (0.1% formic acid in acetonitrile (v/v)) to 40% solvent B over 90 min. Instrument settings for the MS analysis were as follows: capillary voltage of 3.2 kV, cone voltage of 20 V, collision energy of 6.0 V, and source temperature of 80 °C. Mass spectra were acquired over the mass range 200–2000 Da. For calibration, an orthogonal reference spray (LockSpray) of a solution of Glu1-Fibrinopeptide B (500 fmol/μl) in water/acetonitrile (80:20, v/v) and 0.1% formic acid, having a reference mass of 785.8496 (2+) was used. In order to identify glycosylation sites in type I collagen, LC-tandem mass spectrometry (MS/MS) analyses with data-dependent acquisition of the four most abundant ions was employed. A collision energy ramp from 30 to 40 V was employed. To determine the relative levels of Lys, Hyl, G-Hyl, and GG-Hyl for each observed glycosylation site, triplicate LC-MS analyses were acquired.

LC-NanoChip-ESI Ion Trap MS—LC-nanoChip-ESI ion trap MS analyses were performed using an Agilent 6340 XCT Ultra Ion Trap (Santa Clara, CA) equipped with an HPLC Chip Cube MS interface, an Agilent 1100/1200 nanoHPLC System, and an electron transfer dissociation module. Ion trap-MS/MS analyses were performed as follows. 20-μl injections of the tryptic digests dissolved in 0.1% formic acid were loaded onto a 40-nl enrichment column followed by a 43 mm × 75-μm analytical column, packed with ZORBAX 300SB C18 particles (Agilent, Santa Clara, CA). Linear gradients of 3–50% (0.1% formic acid) were performed over 50 min at a flow rate of 500 nl/min. The parameter settings for positive ion ESI-MS were as follows: capillary voltage, 2000 V; end plate offset, 500 V; capillary exit, 180 V; nebulizer, 2 p.s.i., dry gas, 4 liters/min; dry gas temperature, 325 °C. For MS/MS, electron transfer dissociation (ETD) or collision-induced dissociation, automated data-dependent acquisitions of the six most abundant ions were employed. For collision-induced dissociation, the fragmentation amplitude was 0.80 V. For ETD analyses, the accumulation time of the fluoranthene gas was 40 ms, and the reaction time was typically 100 or 150 ms.

Data Analysis—The LC-MS/MS and LC-MS data were visualized with the MassLynx software, version 4.1 (Waters, Milford, MA). Tryptic peptides containing Lys residues and their hydroxylated and/or glycosylated forms were identified from the LC-MS/MS analyses of tryptic digests using manual interpretation of the MS/MS spectra. Relative quantitation of Lys, Hyl, G-Hyl, and GG-Hyl at a particular glycosylation site was performed by dividing the total ion abundance determined for each species by the sum of the ion abundances of all observed species containing that particular site. For example, the ion abundance for G-Hyl was determined by summing up the ion abundances determined for each observed charge state of the multiply protonated glycopeptide ion over the chromatographic elution time of the G-Hyl glycopeptide. For those instances where a modified site was observed as both enzymatically fully processed and as peptides containing one miscleavage, both species were considered in the determination of the ion abundance of that modification. The tryptic peptides and the observed modifications considered for relative quantitation are summarized in supplemental Table 1.

Expression of Lysyl Oxidase Family

MC, EV, and Sh clones were plated at a density of 2×10^5 cells/35-mm dish. After 48 h of culture, total RNA was

extracted with TRIzol reagent (Invitrogen), and 2 μg of total RNA was converted into cDNA by using the Omniscript Reverse Transcriptase kit (Qiagen, Valencia, CA). Quantitative real-time PCR was performed using the sequence-specific primer for lysyl oxidase (LOX) (*Lox*; ABI assay number: Mm00495386_m1), LOXL (*Loxl*; Mm01145738_m1), LOXL2 (*Loxl2*; Mm00804740_m1), LOXL3 (*Loxl3*; Mm00442953_m1), LOXL4 (*Loxl4*; Mm00446385_m1). The reactions were prepared and analyzed in triplicates by the ABI Prism 7000 Sequence detection system (Applied Biosystems, Foster city, CA). The mRNA expression level of LH3 relative to glyceraldehyde 3-phosphate dehydrogenase (GAPDH; ABI assay number 4308313) was analyzed by the $2^{-\Delta\Delta}C_T$ method (46).

Collagen Cross-link Analysis

MC, Sh (Sh1-1, Sh1-2, and Sh1-3) and EV clones were cultured in α-minimum essential medium (Invitrogen) containing 10% fetal bovine serum (FBS; Invitrogen) and 50 μg/ml ascorbic acid. After 2 weeks of culture, cells/matrices were scraped, thoroughly washed with phosphate-buffered saline (PBS) and cold deionized distilled water, and lyophilized. The samples were prepared for collagen cross-link analysis as described previously (47). Briefly, ~2 mg of dried samples was suspended in 0.15 M *N*-trismethyl-2-aminoethanesulfonic acid and 0.05 M Tris-HCl buffer (pH 7.4) and reduced with standardized NaB^3H_4. The specific activity of NaB^3H_4 was determined by the method we reported previously (48). After flushing with N_2, the reduced samples were hydrolyzed with 6 N HCl *in vacuo* at 110 °C for 22 h, and then they were dried, dissolved in distilled water, and filtered. An aliquot of the hydrolysate was subjected to amino acid analysis to determine hydroxyproline content, and the hydrolysates with known amounts of hydroxyproline were analyzed for cross-links on a cation exchange column (AA-911, Transgenomic, Omaha, NE) linked to a fluorescence detector (FP1520, Jasco Spectroscopic, Tokyo, Japan) and a liquid scintillation analyzer (500TR series, Packard Instrument Co., Meriden, CT) as described previously (47). The cross-link precursor aldehydes (*i.e.* hydroxylysyl aldehyde and lysyl aldehyde) and the major reducible cross-links (dehydrodihydroxylysinonorleucine/its ketoamine (deH-DHLNL), dehydrohydroxylysinonorleucine/its ketoamine (deH-HLNL)), were analyzed as their reduced forms (*i.e.* dihydroxynorleucine (DHNL), hydroxynorleucine (HNL), DHLNL, and HLNL, respectively). Hereafter, the terms DHNL, HNL, DHLNL, and HLNL will be used for both the unreduced and reduced forms. The levels of the mature non-reducible cross-links, pyridinoline (Pyr) and deoxypyridinoline were measured with the fluorescence detector and quantified (47). All cross-links and precursor aldehydes were quantified as moles per mole of collagen (48).

Because the *O*-glycosidic linkage of the carbohydrate remains intact in base hydrolysis, the glycosylated immature bifunctional cross-links (GG-DHLNL, G-DHLNL, GG-HLNL, or G-HLNL) were analyzed by subjecting the reduced cells/matrices to base hydrolysis with 2 N NaOH as described previously (42). The pH of the hydrolysate was then adjusted to ~3 with 2 N HCl, and filtered. By applying the hydrolysates to the HPLC system described above, the reducible, glycosylated, and non-glycosylated cross-links were separated. The glycosylated cross-links were identified as described previously (49) with some modifications. Briefly, the base hydrolysates were subjected to partial hydrolysis with 0.2 N and 2 N HCl at 110 °C for 6 h, to stoichiometrically convert the GG- and G- to deglycosylated cross-links, and the respective forms were identified by HPLC. The glycosylated (GG- and G-) and non-glycosylated cross-links were quantified as moles/mole of collagen based on the total values of the cross-links obtained from the acid hydrolysates and the ratio of the respective forms obtained from the base hydrolysates. As for the mature trivalent cross-link, Pyr, a minor cross-link at 2 weeks of culture, its glycosylated forms were not quantified because at least 90% of Pyr cross-links were destroyed by base hydrolysis (50).

In Vitro Collagen Cross-link Maturation Assay

The cell/matrix layers of MC, EV, and Sh clones were collected at 2 weeks of culture, washed, and lyophilized. Several ~2-mg aliquots from each group were dispensed in scintillation vials, suspended in 1 ml of PBS supplemented with 0.7 mM β-aminopropionitrile and two drops of toluene, and sealed. They were then incubated in the dark at 37 °C. At the end of 2 and 4 weeks of incubation, the samples were removed, reduced with standardized NaB^3H_4, hydrolyzed with 6 N HCl, and subjected to cross-link analysis as described above. The non-incubated cell/matrix layers served as the sample at week 0.

Measurements of Collagen Fibril Diameter

MC, EV, and Sh clones were cultured in 35-mm culture dishes, containing α-minimum essential medium, 10% FBS, 100 units/ml penicillin, 100 μg/ml streptomycin, 50 μg/ml ascorbic acid, and 2 mM β-glycerophosphate, for 2 weeks. The cell/matrix layers were then washed with PBS, fixed with 2.5% EM grade glutaraldehyde in 0.1 M sodium cacodylate buffer, pH 7.4. The samples were postfixed in potassium ferrocyanide-reduced osmium for 1 h, dehydrated with a graded series of ethanol concentrations, and embedded in PolyBed-812 epoxy resin (Polysciences, Warrington, PA). Sections of 70 nm were cut, mounted on copper Formvar-carbon filmed grids, and stained with 4% uranyl acetate and Reynolds' lead citrate (51). Cross-sectional views of the collagen fibrils were observed using a LEO EM-910 transmission electron microscope operating at 80 kV (Carl Zeiss SMT, Peabody, MA), and images were taken at 25,000× using a Gatan Orius SC1000 CCD camera with Digital Micrograph 3.11.0 (Gatan, Inc., Pleasanton, CA). For each sample, 1200 fibrils were randomly selected, and the diameters were measured using ImageJ 1.44p software (National Institutes of Health, Bethesda, MD).

In Vitro Mineralization Assay

MC, EV, and Sh clones were plated at a density of 2×10^5 cells/35-mm dish and cultured in α-minimum essential medium containing 10% FBS, 100 units/ml penicillin, and 100 μg/ml streptomycin. Upon confluence, cells were maintained in the mineralization medium containing 50 μg/ml ascorbic acid and 2 mM β-glycerophosphate and cultured for up to 4 weeks. At the end of each week, the cell/matrix layer from each sample were washed with PBS, fixed with 100% methanol, and

stained with 1% Alizarin Red S (Sigma-Aldrich), which binds to calcium in the mineralized nodules deposited (52–54). The rate and the extent of mineral deposition among the clones with varying levels of LH3 enzyme were compared. In addition, at 4 weeks of culture, the extent of mineralization was evaluated from the triplicate measurements of the Alizarin Red S content by using the method reported previously (55).

Statistical Analyses

Statistical analyses were performed using Jmp®8.0 software (SAS Institute Inc., Cary, NC). Statistical differences were determined by Kruskal-Wallis one-way analysis of variance and means comparison by Student's *t* test. The data were presented as means ± S.D., and a *p* value less than 0.05 was considered significant.

TABLE 1

Summary of specific molecular loci and site occupancy of Lys residue modifications in purified type I collagen from MC, EV, and Sh clone, determined by mass spectrometry

Molecular loci (chain-residue no.)	Modification type	Site occupancy		
		MC	Sh	EV
		%	%	%
α1-87	Lys	ND[a]	ND	ND
	Hyl	1.1 ± 0.9	4.6 ± 0.2	1.5 ± 1.3
	G-Hyl	4.2 ± 3.7	60.8 ± 1.2	5.9 ± 1.3
	GG-Hyl	94.7 ± 4.6	34.6 ± 1.3	92.6 ± 0.6
α1-174	Lys	29.2 ± 1.3	38.0 ± 0.8	34.8 ± 1.1
	Hyl	55.4 ± 2.8	51.5 ± 1.0	40.7 ± 0.9
	G-Hyl	11.7 ± 1.8	9.6 ± 1.3	11.8 ± 1.2
	GG-Hyl	3.7 ± 0.4	0.8 ± 0.4	12.8 ± 0.9
α2-87	Lys	4.1 ± 0.3	3.7 ± 0.2	4.6 ± 0.3
	Hyl	89.2 ± 0.9	88.3 ± 0.5	84.0 ± 0.5
	G-Hyl	0.9 ± 0.2	5.8 ± 0.2	0.8 ± 0.1
	GG-Hyl	5.8 ± 0.4	2.1 ± 0.2	10.7 ± 0.2
α2-174	Lys	12.1 ± 2.4	7.9 ± 0.7	24.6 ± 0.4
	Hyl	9.4 ± 1.4	10.2 ± 0.5	4.8 ± 0.1
	G-Hyl	52.7 ± 2.5	75.2 ± 1.2	33.5 ± 0.3
	GG-Hyl	25.8 ± 1.5	6.7 ± 0.2	37.1 ± 0.5
α2-219	Lys	14 ± 1.4	18.5 ± 1.1	20.6 ± 1.6
	Hyl	75.0 ± 5.8	68.1 ± 2.3	52.6 ± 1.7
	G-Hyl	3.5 ± 2.3	9.8 ± 1.7	3.7 ± 0.6
	GG-Hyl	7.5 ± 4.4	3.5 ± 0.3	23.1 ± 2.6

[a] ND, not detected.

RESULTS

Identification of Glycosylation Sites, Form and Extent in Mouse Type I Collagen, and the Effect of LH3 Suppression—For glycopeptide analysis, the trypsinized α1 and α2 chains were analyzed by nanoAcquity UPLC-ESI-QTof Premier MS. Alternatively, the tryptic digests were analyzed by HPLC-nanoESI ion trap equipped with ETD capabilities. The QTof MS and MS/MS spectra were acquired using data-dependent acquisition of the four most abundant precursor ions, whereas on the ion trap, selection of six precursor ions was employed. The glycopeptides α1(76–90) containing the glycosylated residue Hyl-87 were observed as triply protonated ions of *m*/*z* 558.949 and 612.971, corresponding to glycoforms of G-Hyl and GG-Hyl, respectively. The nonhydroxylated Lys was not detected in this peptide (Table 1), indicating that this residue is quantitatively hydroxylated. The extracted ion chromatograms (*EIC*) of the two ions in the α1 tryptic digests isolated from the MC and Sh collagen are shown in Fig. 1. In the MC α1 tryptic digest, the predominant glycoform was assigned to peptide 76–90 with residue 87 in the form of GG-Hyl (Fig. 1*A*) with minimal abundance of the G-Hyl glycoform (Fig. 1*B*). Structural characterization of glycopeptide ions *m*/*z* 612.7 (3+) and 558.7 (3+) by ETD confirmed the assignment as α1(76–90) containing GG-Hyl and G-Hyl, based on the presence of fragment ions arising from cleavage of the N–Cα bond retaining the glycan moiety (Fig. 2). In contrast, in the α1 chain isolated from the Sh collagen, the most abundant glycoform at residue 87 was G-Hyl, whereas GG-Hyl was found with significantly lower relative abundance compared with MC (Fig. 1, *C* and *D*).

In contrast to α1-87, Lys-87 on the α2 chain was found modified mainly by Lys hydroxylation in peptide 76–87 ($M_{r(exp)}$ =

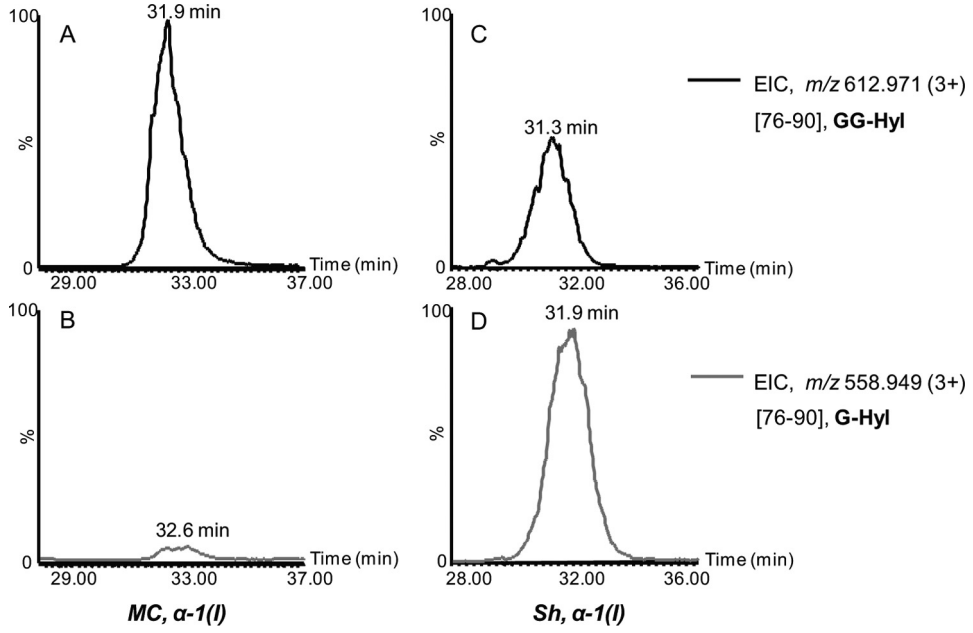

FIGURE 1. **Extracted ion chromatograms (*EIC*) of triply protonated ions of *m/z* 612.971 and 558.949, corresponding to glycopeptides α-1(I)(76–90), containing GG-Hyl and G-Hyl, respectively.** *A* and *B*, MC collagen; *C* and *D*, Sh collagen. For each collagen sample, the extracted ion chromatograms were normalized to the abundance of the most abundant glycoform.

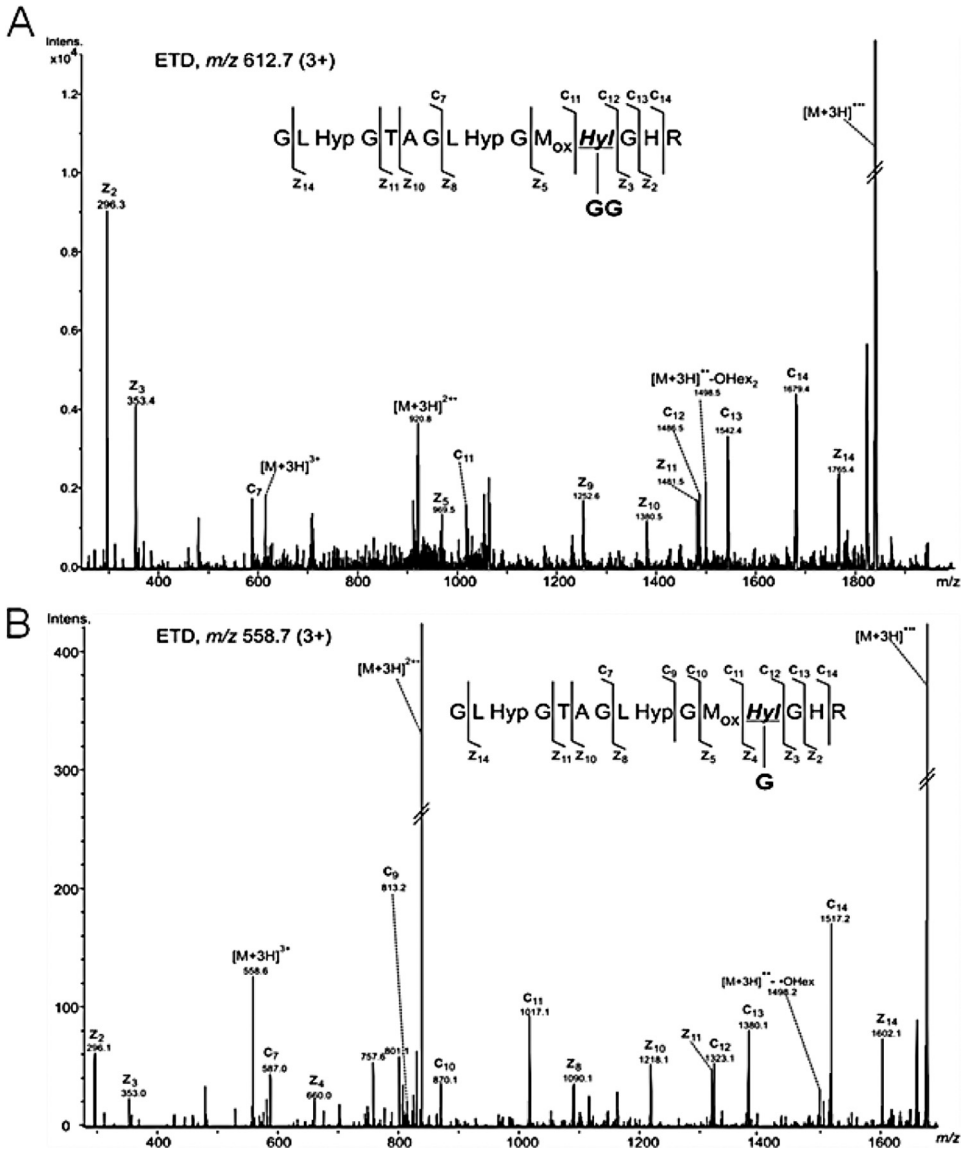

FIGURE 2. **Structural characterization of α1(I) glycopeptides 76–90.** Shown are ETD spectra acquired on the ion trap of the ions of *m/z* 612.7 (3+) (*A*) and *m/z* 558.7 (3+) (*B*), corresponding to the α1(I) glycopeptides 76–90 containing GG-Hyl, and G-Hyl, respectively. *G*, one hexose unit; *GG*, two hexose units.

1237.578) with minimal amounts of GG-Hyl and G-Hyl (Table 1 and supplemental Table 1 and Fig. 1).

Furthermore, the residues α1-174 and α2-174 were found modified by various levels of hydroxylation and glycosylation. In type I collagen isolated from MC, the major modification observed at residue α1-174, accounting for 55.4% of the site occupancy, was Lys hydroxylation, whereas glycosylation of Hyl 174 accounts only for a relatively small amount of modification (see Table 1). Within the glycosylated structures, G-Hyl ($M_{r(exp)}$ = 3576.733, relative abundance 11.7%) was found to be higher than GG-Hyl ($M_{r(exp)}$ = 3738.823, relative abundance 3.7%). In the collagen purified from the Sh clone, higher relative amounts of free Lys were found compared with MC (38% in Sh *versus* 29.2% in MC), whereas the levels of GG-Hyl in Sh collagen were decreased (0.8% in Sh *versus* 3.7% in MC). In contrast to α1-174, higher levels of modification were observed at residue α2-174 (Table 1), because the unmodified Lys accounted for only 12% of this site. Residue α2-Hyl-174 was found to have higher levels of glycosylation compared with α1-Hyl-174, and within the glycosylated forms, G-Hyl ($M_{r(exp)}$ = 4363.177, relative abundance 52.7%) was higher than that of GG-Hyl ($M_{r(exp)}$ = 4525.063, relative abundance 25.8%). The identities of these glycopeptides were confirmed by MS/MS (data not shown). As a result of the LH3 suppression, higher relative amounts of G-Hyl and lower amounts of GG-Hyl were identified at residue α2-174 as well, whereas the relative levels of Lys and Hyl did not change significantly (see Table 1).

In MC collagen, one additional glycosylation site was identified at residue α2-219, minimally occupied with GG-Hyl and G-Hyl, whereas the major modification was assigned to Hyl (see Table 1). It is noteworthy that, unlike residues α1-174 and α2-174, the relative abundance of GG-Hyl (relative abundance 7.5%) was found to be higher than that of G-Hyl (relative abundance 3.5%). The homologous residue α1-219 was largely observed as Lys or Hyl, whereas no glycosylated structures of this residue were detected.

TABLE 2

Levels of immature reducible cross-links (HLNL, DHLNL, and its glycosylated forms) and mature non-reducible cross-links (Pyr) from MC, EV, and Sh clones

Values represent mean (S.D. in parentheses) from three independent experiments.

Cells/Clones	Total DHLNL[a]	GG-DHLNL	G-DHLNL	DHLNL	HLNL	Pyr	Total aldehydes[b]
	mol/mol collagen	*mol/mol collagen*	*mol/mol collagen*	*mol/mol collagen*	*mol/mol collagen*	*mol/mol collagen*	*mol/mol collagen*
MC	1.081 (0.26)	0.480 (0.07)	0.050 (0.02)	0.551 (0.17)	0.210 (0.03)	0.047 (0.008)	1.39 (0.24)
Sh1-1	0.690 (0.07)[c]	0.223 (0.01)[c]	0.134 (0.02)[c]	0.333 (0.04)[c]	0.170 (0.02)[d]	0.026 (0.005)[c]	0.91 (0.07)[c]
Sh1-2	0.657 (0.03)[c]	0.171 (0.01)[c]	0.132 (0.01)[c]	0.353 (0.01)[c]	0.155 (0.05)[c]	0.023 (0.005)[c]	0.85 (0.01)[c]
Sh1-3	0.663 (0.08)[c]	0.200 (0.03)[c]	0.143 (0.05)[c]	0.320 (0.01)[c]	0.169 (0.02)[d]	0.016 (0.005)[c]	0.88 (0.10)[c]
EV	1.056 (0.26)	0.443 (0.09)	0.047 (0.05)	0.565 (0.12)	0.236 (0.01)	0.044 (0.018)	1.38 (0.30)

[a] Total DHLNL = GG-DHLNL + G-DHLNL + non-glycosylated DHLNL.
[b] Total aldehydes = total DHLNL + HLNL + 2× Pyr.
[c] Significantly different from both controls MC and EV.
[d] Significantly different from EV ($p < 0.05$).

Table 1 summarizes the percentages of site occupancy of Lys, Hyl, G-Hyl, and GG-Hyl, in type I collagen purified from MC, Sh, and EV clones, as determined by MS analyses. From the LC-MS/MS data, peptide heterogeneity might arise from the following: partial hydroxylation and glycosylation of Lys and Hyl residues, respectively, partial proline hydroxylation, methionine oxidation, and trypsin miscleavage at the C terminus to the modified Lys. As expected, trypsin proteolysis after glycosylated Hyl was completely abolished, as evidenced from the observation of glycosylated peptides never containing G- or GG-Hyl at their C termini. In contrast, cleavage C-terminal to non-glycosylated Hyl still occurs, whereas the rate of cleavage appeared to be peptide-specific. Presumably, the substrate specificity in the Hyl-containing collagen peptides may be affected by neighboring amino acids. The peptides and their modifications considered for the site-specific, relative quantitation of glycosylation are shown in supplemental Table 1. Collectively, the results show that in the Sh collagen, the relative abundance of GG-Hyl is decreased at all of the identified glycosylated sites with concomitant increases in the levels of G-Hyl. The only exception was α1-174 where the relative abundance of G-Hyl did not increase in the Sh clone. The data shown here are consistent with the previously reported HPLC analysis of the collagen from MC, EV, and Sh clones (12) and confirm the function of LH3 as a glucosyltransferase enzyme.

Because the major glucosylation site (α1-87) is one of the major intermolecular cross-linking sites of type I collagen in mineralized tissues (38, 39, 56–58), its potential effects on cross-linking were further examined.

Collagen Cross-link Analysis—The collagen cross-links produced by MC, EV, and Sh clones at 2 weeks of culture were composed mainly of reducible, immature bifunctional cross-links, DHLNL and HLNL, and a small amount of mature trifunctional cross-link (Pyr). Deoxypyridinoline was not detected in any of those culture samples. The levels of free precursor aldehydes, DHNL and HNL, were minimal (<0.01 mol/mol of collagen). The amounts of DHLNL, HLNL, Pyr, and the total number of aldehydes involved in cross-linking (DHLNL + HLNL + 2× Pyr) are depicted in Table 2. The major immature cross-link, total DHLNL (GG-, G-, and non-glycosylated DHLNL), and a mature cross-link, Pyr, in all three LH3-Sh clones (Sh1-1, -2, and -3) were significantly lower than those of controls ($p < 0.05$). The total numbers of aldehydes were also significantly lower in the Sh clones when compared with both controls ($p < 0.05$). Fig. 3 shows the typical chromatographic pattern of the base hydrolysates obtained from MC, Sh, and EV clones, indicating glycosylated (GG- and G-DHLNL) and non-glycosylated (DHLNL and HLNL) cross-links. The percentages of glycosylated (GG- and G-) and non-glycosylated forms of DHLNL are also indicated. The relative amounts of HLNL were unchanged with base hydrolysis, indicating that it is not glycosylated. Approximately one-half of total DHLNL, however, was found to be glycosylated in all groups. Of the glycosylated forms, the relative amounts of GG-DHLNL in all Sh clones were diminished with concomitant increases in G-DHLNL, when compared with both control groups. The levels of these various forms of DHLNL were quantified as moles/mole of collagen, using the total amounts of DHLNL determined from the acid hydrolysates and their relative ratio, and they are shown in Table 2. From the Sh clones, there were significant decreases in the levels of free DHLNL and GG-DHLNL ($p < 0.05$) with concomitant increases in the levels of G-DHLNL ($p < 0.05$) when compared with the controls, MC and EV. In the case of HLNL, only Sh1-2 was significantly lower than that in both MC and EV, whereas Sh1-1 and Sh1-3 were significantly lower than EV only.

Expressions of Lysyl Oxidase and Its Isoforms—Because the amounts of cross-links/total aldehydes were significantly lower in all Sh clones, we then examined the potential effects of LH3 suppression on the gene expression of LOX, an enzyme responsible for the initiation of cross-linking, and its isoforms (LOXL and LOXL2 to -4). However, real-time PCR analyses from three independent experiments showed that the expression of *Lox*, *Loxl*, and *Loxl2* to *-4* in the Sh clones were essentially identical to those in the controls, except for the expression of *Lox* in Sh1-1, which is comparable with MC but slightly lower than EV ($p = 0.0359$) (supplemental Fig. 2). The expression of *Loxl2* was not detected in both the controls and Sh clones, thus consistent with our previous report (59).

In Vitro Cross-link Maturation Assay—It has been proposed that Pyr is a maturational product from the condensation reaction between two deH-DHLNL/its ketoamine residues (60, 61). Thus, to assess the potential effect of glycosylation on the cross-link maturation, we have utilized the cell-free *in vitro* cross-link maturation assay. This system allows us to directly measure the amounts of the precursor (deH-DHLNL) and the product (Pyr) during the incubation period. Fig. 4 shows the changes in the levels of DHLNL and Pyr over time (weeks 0, 2, and 4).

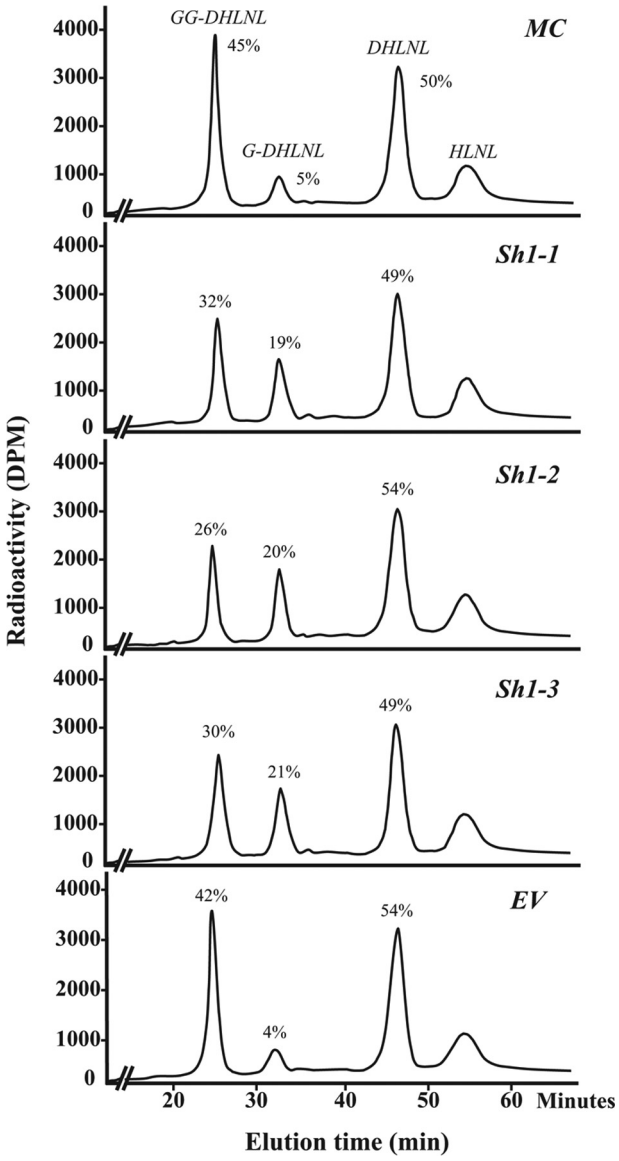

FIGURE 3. **Glycosylation of reducible collagen cross-links obtained from MC, EV, and Sh clones at 2 weeks of cell culture.** The base hydrolysates of NaB^3H_4-reduced cells/matrices were analyzed by HPLC. The amounts of GG-, G-, and DHLNL are shown in percentages (GG-DHLNL + G-DHLNL + DHLNL = 100%). Note the decrease in GG-DHLNL with concomitant increase in G-DHLNL in the Sh clones, when compared with controls, MC and EV. No glycosylation was detected for HLNL.

Although the values of the cross-links at week 2 showed some variation within the groups, those at week 4 were similar to one another (*i.e.* for DHLNL, 0.20 ± 0.01 and 0.18 ± 0.02, and for Pyr, 0.23 ± 0.01 and 0.26 ± 0.04, in controls and Sh clones, respectively. In Sh clones, on average, DHLNL was diminished from 0.7 ± 0.04 at week 0 to 0.2 ± 0.02 mol/mol of collagen at week 4, and Pyr increased from 0.03 ± 0.004 at week 0 to 0.26 ± 0.04 mol/mol of collagen at week 4. In controls (MC and EV), on average, the former decreased from 1.4 ± 0.01 to 0.2 ± 0.02, and the latter increased from 0.06 ± 0.01 to 0.23 ± 0.01 mol/mol of collagen. Thus, although the increase of Pyr was comparable between the Sh clones and controls, the rate of decrease in DHLNL was significantly greater in controls when compared with that of Sh clones. Three independent incubations were performed, and the results were reproducible.

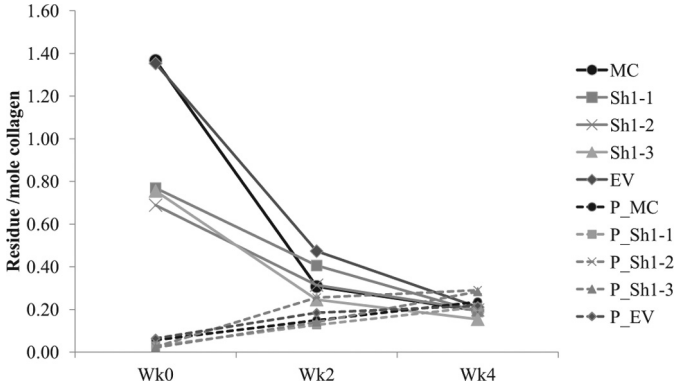

FIGURE 4. ***In vitro* cross-link maturation assay.** 2 mg of lyophilized cells/matrices from MC, EV, and the Sh clones were incubated (for details, see "Experimental Procedures"). At weeks 2 and 4 of incubation, the samples were reduced with NaB^3H_4 and analyzed for the levels of immature reducible (DHLNL) and mature non-reducible (Pyr) cross-links. The changes in DHLNL are shown with *solid lines*, and those of Pyr are shown with *dotted lines*.

Characterization of Collagen Fibrils by Transmission Electron Microscopy—Cross-sectional views of collagen fibrils and the diameter distribution obtained from the cultures of Sh clones (Sh1-1, -2, and -3) and the controls (MC and EV clone) are shown in Fig. 5. The fibrils from the controls and Sh clones are generally circular in shape. The fibril diameters were measured from 1200 randomly selected fibrils of each group. EV showed a slightly larger mean and range of collagen fibril diameter than those of MC ($p < 0.05$), as seen in the *in vitro* fibrillogenesis assay (12). The slight phenotypic difference between EV and MC, possibly due to the transfection effect, has also been reported in other studies (52, 54). In all of the Sh clones, the mean fibril diameters and their ranges were significantly larger when compared with those of the controls, MC and EV ($p < 0.05$). The order of the means of fibril diameters from the smallest to the largest is as follows: MC < EV < Sh1-1 < Sh1-3 < Sh1-2. The results shown here are consistent with the turbidity-time curve from the *in vitro* fibrillogenesis assay, using purified type I collagen from the Sh clones and the controls (12).

In Vitro Matrix Mineralization Assay—The results of *in vitro* mineralization assay, by Alizarin Red staining, are shown in Fig. 6. In the controls, MC and EV, the formation of mineralized nodules, was already observed at 2–3 weeks of culture and gradually increased in the number and size of the nodules overtime. On the contrary, matrix mineralization in the Sh clones was significantly delayed. Sh1-1 and -2 showed almost no nodules for up to 4 weeks of culture. Sh1-3 showed a few nodules at week 3, and they increased at week 4 (Fig. 6*A*). The quantitative analyses of Alizarin Red S content at week 4 demonstrated that the extents of mineralization in all Sh clones were significantly less than those of MC and EV ($p < 0.05$) (Fig. 6*B*).

DISCUSSION

The glycosylation of type I collagen has been investigated in the past 45 years, and several molecular loci were identified in various tissues and species (62–66). However, to the best of our knowledge, this is the first study to systematically identify the specific molecular loci and forms of Hyl glycosylation in type I collagen in any cell culture system. Five specific Hyl residues in type I collagen were found to be glycosylated, and they are

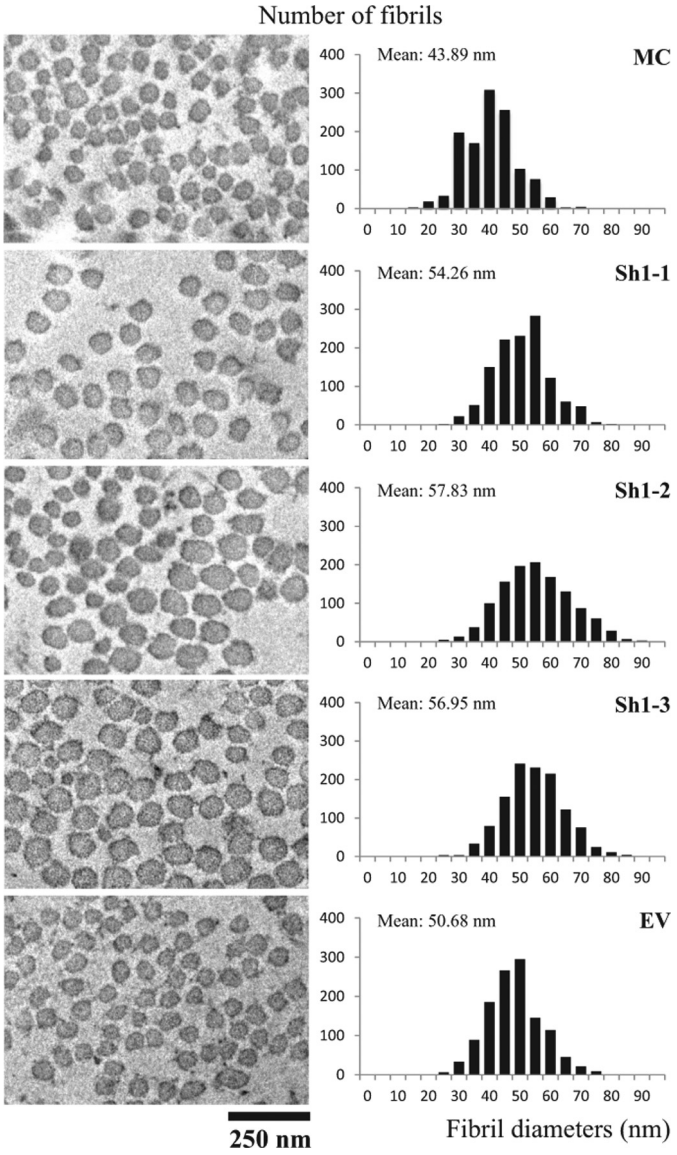

FIGURE 5. **Ultrastructural analysis of collagen fibrils in cell cultures.** The cells/matrices were collected from MC, EV, and Sh clones after 2 weeks of culture, and the cross-section of the collagen fibrils was observed under a transmission electron microscope. The images were taken at a magnification of ×25,000 using Gatan's Digital Micrograph software. Fibril diameters were measured using ImageJ 1.44p software, and the diameter distribution was plotted based on the total number of 1200 fibrils per clone and is shown on the *right*.

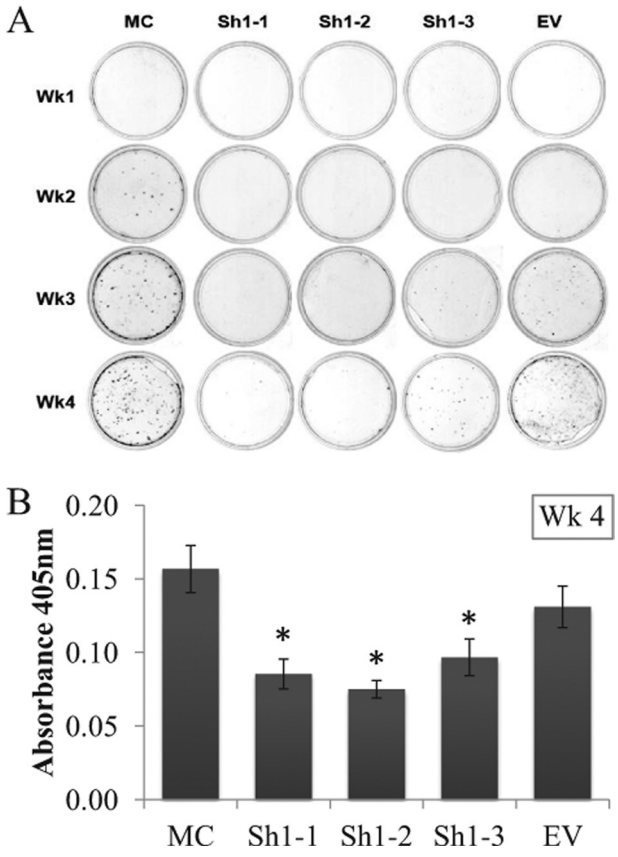

FIGURE 6. ***In vitro* mineralization assay.** *A*, MC, EV, and Sh clones were cultured in mineralization medium for 1, 2, 3, and 4 weeks. At the end of each week, the cells/matrices were stained with Alizarin Red S. *B*, Alizarin Red S contents of Sh clones and controls. The contents were measured by absorbance at 405 nm at 4 weeks of culture. *Error bars*, S.D. of triplicate measurements. *, significantly different ($p < 0.05$) from MC and EV. *Wk*, week.

α1-Hyl-87, α1-Hyl-174, α2-Hyl-87, α2-Hyl-174, and α2-Hyl-219, which is consistent with those previously identified in other species (62–66). At these sites, the glycosylation pattern was significantly different between α1 and α2 chains. In the α1 chain, α1-87 was almost fully hydroxylated and glycosylated, whereas its homologous site on the α2 chain contains only trace amounts of glycosylation. For residue 174, only ~15% was glycosylated in the α1 chain, whereas it was nearly 80% in the α2 chain. In addition, both G- and GG-Hyl forms were identified at α2-219, but none of these was detected at α1-219. The reason for this differential glycosylation pattern between α1 and α2 chains is not clear at this point. It is of interest to note that the Hyl residue α2-87 in bovine periodontal ligament (42) and bovine bone[3] type I collagen is mostly glycosylated. By comparing the amino acid sequences of the α1 and α2 chains near the identified glycosylation sites among different species (*e.g.* human mouse, rat, and bovine), it is apparent that in the α1 chain, there is a higher degree of sequence homology around the Lys residues that were hydroxylated and glycosylated (*i.e.* residues 87, 174, and 219 (α1 chain: sequence accession numbers P02452, P11087, P02454, and P02453, respectively). The sequence comparison of α2 chain, however, showed some differences adjacent to the Lys 87 between the mouse and other species (GFKGVK *versus* GFKGIR) but not at residues 174 and 219 (α2 chain: sequence accession numbers P08123, Q01149, P02466, and P02465, respectively). The variation in the amino acid sequences among the different species probably resulted in the varied levels of glycosylation between the homologous sites on α1 and α2 chains, as shown by MS analyses. Collectively, these results, along with the differences in the amino acid sequence among the species or the α chains, may implicate sequence-specific preference for the glycosyltransferase enzymes.

When LH3 was suppressed, the levels of GG-Hyl were greatly diminished at all of the identified sites with concomitant

[3] M. Terajima, I. Perdivara, M. Sricholpech, K. B. Tomer, and M. Yamauchi, unpublished observations.

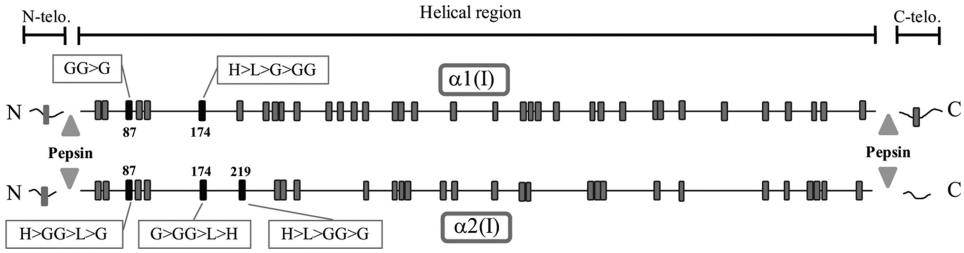

FIGURE 7. **Molecular loci of glycosylated hydroxylysine residues in α1(I) and α2(I) chains of type I collagen synthesized by MC3T3-E1 cells.** Note that the glycosylated Hyl residues were identified exclusively in the N-terminal helical region of the α chains and that the extent of the modifications varies depending on the locus. *telo*, telopeptide; *L*, lysine; *H*, hydroxylysine; *G*, galactosylhydroxylysine; *GG*, glucosylgalactosylhydroxylysine. *Gray squares*, lysine or hydroxylysine residues; *black squares*, glycosylated hydroxylysine residues.

increases in G-Hyl at four of the five sites (Table 1). These results clearly demonstrate that in the mouse osteoblast culture system, 1) glycosylation occurs at specific sites in type I collagen, 2) LH3 functions as glucosyltransferase for all of the identified sites, and 3) the extent and type of glycosylation vary in a site-specific manner, but the residue α1-87 appears to be fully hydroxylated and glycosylated mostly in the form of GG-Hyl. The distribution of Lys in the α1 and α2 chains, the glycosylation sites, and relative abundance of the modifications identified are shown in Fig. 7. Interestingly, all of the glycosylation sites identified are located in the N-terminal side of the helical domain of the collagen molecule. The heterogeneity of the modifications at each site could be attributed to its specific function in which further investigation is warranted. It is noteworthy that the most predominant glycosylated site, α1-87, is one of the major helical cross-linking sites in type I collagen (56, 57).

There are several unique features of collagen cross-linking in mineralized tissues that are thought to be important to control the spatial aspect of mineralization, including the chemical state of the α1-16^{C} in the C-telopeptide that cross-links to the juxtaposed helical α1/2-87 (48, 56, 57). However, the role of the glycosylation at the latter residues on cross-linking is not known. Considering the MS data indicating that the helical α1-87 is almost fully glycosylated and the other helical cross-linking Hyl (α1–930/α2–933) are not glycosylated (Table 1; see "Results"), it is likely that the glycosylated DHLNL is derived from α1-16^{C} × α1-87 (*i.e.* α2-87 is mostly non-glycosylated). By applying the tryptic digests of the NaB^{3}H$_{4}$ reduced cells/matrices to our standardized column chromatography (42, 56), we estimated that ~80% of the DHLNL cross-link in the current cell culture system is derived from α1-16^{C} × α1/2-87 (data not shown), which is consistent with the previous data on bone collagen (56). Some of the non-glycosylated DHLNL could be derived from α1-16^{C} × α2-87 and the N-telopeptide α1-9^{N}/α2-5^{N} × helical α1-930/α2-933. The precise glycosylation state of each site needs to be determined by isolation of the peptides followed by MS analysis. As for HLNL, in both Sh clones and controls, no significant glycosylation was found. This is probably due to the fact that the majority of the HLNL cross-link is derived from hydroxylysyl aldehyde × Lys (67) in mineralized tissues (thus, no glycosylation).

The data indicated the regulatory roles of LH3-mediated glucosylation in collagen cross-linking. In Sh clones, the levels of cross-links (both DHLNL and Pyr) were significantly diminished. Because the gene expression levels of *Lox* and *Loxls* in the Sh clones were comparable with those of controls, the decrease in cross-links could be due to the impaired activity of LOX. It has been reported that LOX is more active toward quarter-staggered, native collagen fibrils, and it has been suggested that the intermolecular interactions between collagen molecules are important for the enzyme activity (68). Studies have also shown that the binding sites for LOX in type I collagen are in the triple helical region (69), potentially in the area with highly conserved sequences (Hyl-Gly-His-Arg, corresponding to the residues 87–90 and 930–933 on α chains), where it can catalyze the formation of Lys or Hyl aldehyde in the juxtaposed C- or N-telopeptides of the adjacent collagen molecule (70). Thus, the decrease in G-Hyl glucosylation at α1-87 of the Sh collagen could affect the binding and/or activity of the LOX enzymes, leading to the diminished level of cross-linking.

The LH3-mediated glucosylation could also play a role in the cross-link maturation. It has been proposed that the bifunctional cross-link, DHLNL, matures into the trifunctional mature cross-link, Pyr, by condensation between two residues of DHLNL/ketoamine (60, 61, 71). However, the stoichiometry between the decrease in DHLNL and the increase in Pyr in a ratio of 2:1 does not always exist. For instance, Eyre *et al.* (72) reported in human bone tissue a fast decrease in the level of immature bifunctional cross-links with age, whereas the level of Pyr formation was disproportionately lower. In the current study, the results of an *in vitro* incubation assay showed that there was a faster decrease in DHLNL in the controls, MC and EV, compared with the Sh clones. The decrease of DHLNL in the former was disproportionately greater than the formation of its maturational product, Pyr. It is of interest to note that if the amounts of GG-DHLNL are not accounted for, the ratio of the decrease of (G-DHLNL + DHLNL) and the increase of Pyr from week 0 to week 4 was close to 2:1 regardless of the cell groups. Therefore, it is possible that the diglycosylated form of DHLNL may not favor the formation of Pyr but may undergo further unknown modifications. Robins and Bailey (73) also suggested the potential role of glycosylation in the DHLNL maturation based on the observation that the rate of disappearance of DHLNL was faster than that of HLNL *in vitro*. In light of this, it is notable that several reports had demonstrated the presence of G-Pyr and free Pyr but not GG-Pyr in bone collagen (39, 40, 74). The putative maturation mechanism of DHLNL into its arginine adduct (75) is less likely in our *in vitro* incubation system because no free arginine is available. Further studies are warranted to elucidate the potential role of glycosylation (its extent as well as its mono- or diglycosylated forms) in the

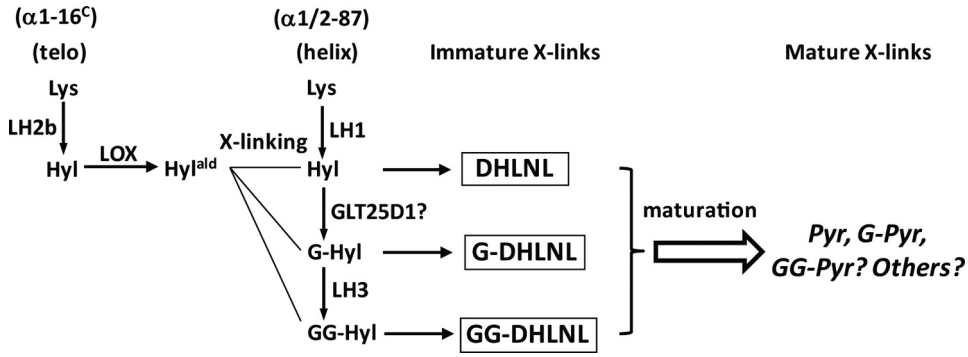

FIGURE 8. **The major cross-linking pathway in MC3T3-E1 culture system.** α*1-16*^{C}, 16th residue from the N terminus of the C-telopeptide of an α1 chain; *telo*, telopeptides; α *1/2-87*, 87th residue from the N terminus of the triple helical domain of the α1 or α2 chain, respectively; *helix*, helical domain of collagen; *LH*, lysyl hydroxylase; *GLT25D1*, glycosyltransferase 25 domain 1; *Hyl*^{ald}, hydroxylysyl aldehyde.

DHLNL cross-link maturation. The major collagen cross-linking pathway involving the C-telopeptide (α1-16^{C}) and the juxtaposed helical α1/2-87 residues in the osteoblast culture system/mineralized tissues is illustrated in Fig. 8.

The decreased level of LH3-mediated glucosylation also leads to altered fibrillogenesis, as determined by transmission electron microscopy. The diameters of collagen fibrils from the Sh clones are significantly larger than those of controls. This result is in agreement with our previous report (12) and others (33, 34, 36, 37) showing that collagen with lower levels of glycosylation forms larger diameter fibrils *in vitro*. On the contrary, Risteli *et al.* (25) have shown that the mean collagen fibril diameters from the skin of adult heterozygous LH3 knock-out mice are significantly smaller than those from the wild type mice. The discrepancy observed may arise from the differences in cell types (*i.e.* osteoblasts *versus* fibroblasts) and their microenvironment.

In the present study, the Sh clones (collagen with low glucosylation) showed delayed mineralization *in vitro*. It is not clear what causes the delay. This could be due to an altered interaction between collagen and non-collagenous proteins important for the initiation of mineralization (54, 76, 77), which could be caused by lower levels of GG-Hyl. Based on the molecular loci of glycosylation identified by MS, the sites are located in close proximity to or in the gap zone, which is the putative site for the initiation of mineralization (78, 79). According to the functional and ligand binding regions mapped in type I collagen, those glycosylation sites are in the binding areas of various matrix proteins (*e.g.* integrins, proteoglycans, phosphophoryn, and discoidin domain receptor 2) (80). Therefore, the glycosylated Hyl residues exclusively in these regions may play a regulatory role in the mineralization process either directly by facilitating the deposition of minerals or indirectly by interacting with non-collagenous proteins. Alternatively, defective connectivity of collagen molecules in the fibril due to the low levels of cross-links may also delay the process of mineralization (48, 57). Further studies are warranted to elucidate the potential roles of collagen glycosylation in mineralization.

In conclusion, this study clearly demonstrates that the LH3-mediated glucosylation occurs at at least five specific sites in type I collagen, the major one being at α1-87, which is involved in intermolecular cross-linking. The suppression of LH3 causes altered cross-link formation, cross-link maturation, fibrillogenesis, and mineralization. These results underscore the critical roles of this post-translational modification in collagen functions.

REFERENCES

1. Shinkai, H., and Yonemasu, K. (1979) Hydroxylysine-linked glycosides of human complement subcomponent C1q and various collagens. *Biochem. J.* **177,** 847–852
2. Miller, E. J. (1984) Collagen Chemistry. in *Extracellular Matrix Biochemistry* (Piez, K. A., and Reddi, A. H., eds) pp. 41–78, Elsevier Science Publishing Co., Inc.
3. Yamauchi, M., and Sricholpech, M. (2012) Lysine post-translational modifications of collagen. *Essays Biochem.* **52,** 113–133
4. Kivirikko, K. I., and Myllylä, R. (1982) Posttranslational enzymes in the biosynthesis of collagen: intracellular enzymes. *Methods Enzymol.* **82,** 245–304
5. Heikkinen, J., Risteli, M., Wang, C., Latvala, J., Rossi, M., Valtavaara, M., and Myllylä, R. (2000) Lysyl hydroxylase 3 is a multifunctional protein possessing collagen glucosyltransferase activity. *J. Biol. Chem.* **275,** 36158–36163
6. Wang, C., Luosujärvi, H., Heikkinen, J., Risteli, M., Uitto, L., and Myllylä, R. (2002) The third activity for lysyl hydroxylase 3. Galactosylation of hydroxylysyl residues in collagens *in vitro*. *Matrix Biol.* **21,** 559–566
7. Schegg, B., Hülsmeier, A. J., Rutschmann, C., Maag, C., and Hennet, T. (2009) Core glycosylation of collagen is initiated by two β(1-*O*)galactosyltransferases. *Mol. Cell. Biol.* **29,** 943–952
8. Rautavuoma, K., Takaluoma, K., Passoja, K., Pirskanen, A., Kvist, A. P., Kivirikko, K. I., and Myllyharju, J. (2002) Characterization of three fragments that constitute the monomers of the human lysyl hydroxylase isoenzymes 1–3. The 30-kDa N-terminal fragment is not required for lysyl hydroxylase activity. *J. Biol. Chem.* **277,** 23084–23091
9. Wang, C., Risteli, M., Heikkinen, J., Hussa, A. K., Uitto, L., and Myllyla, R. (2002) Identification of amino acids important for the catalytic activity of the collagen glucosyltransferase associated with the multifunctional lysyl hydroxylase 3 (LH3). *J. Biol. Chem.* **277,** 18568–18573
10. Rautavuoma, K., Takaluoma, K., Sormunen, R., Myllyharju, J., Kivirikko, K. I., and Soininen, R. (2004) Premature aggregation of type IV collagen and early lethality in lysyl hydroxylase 3 null mice. *Proc. Natl. Acad. Sci. U.S.A.* **101,** 14120–14125
11. Ruotsalainen, H., Sipilä, L., Vapola, M., Sormunen, R., Salo, A. M., Uitto, L., Mercer, D. K., Robins, S. P., Risteli, M., Aszodi, A., Fässler, R., and Myllylä, R. (2006) Glycosylation catalyzed by lysyl hydroxylase 3 is essential for basement membranes. *J. Cell Sci.* **119,** 625–635
12. Sricholpech, M., Perdivara, I., Nagaoka, H., Yokoyama, M., Tomer, K. B., and Yamauchi, M. (2011) Lysyl hydroxylase 3 glucosylates galactosylhydroxylysine residues in type I collagen in osteoblast culture. *J. Biol. Chem.* **286,** 8846–8856
13. Suarez, K. N., Romanello, M., Bettica, P., and Moro, L. (1996) Collagen type I of rat cortical and trabecular bone differs in the extent of posttranslational modifications. *Calcif. Tissue Int.* **58,** 65–69

14. Moro, L., Romanello, M., Favia, A., Lamanna, M. P., and Lozupone, E. (2000) Posttranslational modifications of bone collagen type I are related to the function of rat femoral regions. *Calcif. Tissue Int.* **66,** 151–156
15. Schofield, J. D., Freeman, I. L., and Jackson, D. S. (1971) The isolation, and amino acid and carbohydrate composition, of polymeric collagens prepared from various human tissues. *Biochem. J.* **124,** 467–473
16. Toole, B. P., Kang, A. H., Trelstad, R. L., and Gross, J. (1972) Collagen heterogeneity within different growth regions of long bones of rachitic and non-rachitic chicks. *Biochem. J.* **127,** 715–720
17. Kivirikko, K. I., and Myllylä, R. (1979) Collagen glycosyltransferases. *Int. Rev. Connect Tissue Res.* **8,** 23–72
18. Savolainen, E. R., Kero, M., Pihlajaniemi, T., and Kivirikko, K. I. (1981) Deficiency of galactosylhydroxylysyl glucosyltransferase, an enzyme of collagen synthesis, in a family with dominant epidermolysis bullosa simplex. *N. Engl. J. Med.* **304,** 197–204
19. Michalsky, M., Norris-Suarez, K., Bettica, P., Pecile, A., and Moro, L. (1993) Rat cortical and trabecular bone collagen glycosylation are differently influenced by ovariectomy. *Biochem. Biophys. Res. Commun.* **192,** 1281–1288
20. Tenni, R., Valli, M., Rossi, A., and Cetta, G. (1993) Possible role of overglycosylation in the type I collagen triple helical domain in the molecular pathogenesis of osteogenesis imperfecta. *Am. J. Med. Genet.* **45,** 252–256
21. Lehmann, H. W., Wolf, E., Röser, K., Bodo, M., Delling, G., and Müller, P. K. (1995) Composition and posttranslational modification of individual collagen chains from osteosarcomas and osteofibrous dysplasias. *J. Cancer Res. Clin. Oncol.* **121,** 413–418
22. Brinckmann, J., Notbohm, H., Tronnier, M., Açil, Y., Fietzek, P. P., Schmeller, W., Müller, P. K., and Bätge, B. (1999) Overhydroxylation of lysyl residues is the initial step for altered collagen cross-links and fibril architecture in fibrotic skin. *J. Invest. Dermatol.* **113,** 617–621
23. Dominguez, L. J., Barbagallo, M., and Moro, L. (2005) Collagen overglycosylation. A biochemical feature that may contribute to bone quality. *Biochem. Biophys. Res. Commun.* **330,** 1–4
24. Salo, A. M., Cox, H., Farndon, P., Moss, C., Grindulis, H., Risteli, M., Robins, S. P., and Myllylä, R. (2008) A connective tissue disorder caused by mutations of the lysyl hydroxylase 3 gene. *Am. J. Hum. Genet.* **83,** 495–503
25. Risteli, M., Ruotsalainen, H., Salo, A. M., Sormunen, R., Sipilä, L., Baker, N. L., Lamandé, S. R., Vimpari-Kauppinen, L., and Myllylä, R. (2009) Reduction of lysyl hydroxylase 3 causes deleterious changes in the deposition and organization of extracellular matrix. *J. Biol. Chem.* **284,** 28204–28211
26. Segrest, J. P., and Cunningham, L. W. (1970) Variations in human urinary *O*-hydroxylysyl glycoside levels and their relationship to collagen metabolism. *J. Clin. Invest.* **49,** 1497–1509
27. Pinnell, S. R., Fox, R., and Krane, S. M. (1971) Human collagens. Differences in glycosylated hydroxylysines in skin and bone. *Biochim. Biophys. Acta* **229,** 119–122
28. Brenner, R. E., Vetter, U., Nerlich, A., Wörsdorfer, O., Teller, W. M., and Müller, P. K. (1990) Altered collagen metabolism in osteogenesis imperfecta fibroblasts. A study on 33 patients with diverse forms. *Eur. J. Clin. Invest.* **20,** 8–14
29. Bateman, J. F., Mascara, T., Chan, D., and Cole, W. G. (1984) Abnormal type I collagen metabolism by cultured fibroblasts in lethal perinatal osteogenesis imperfecta. *Biochem. J.* **217,** 103–115
30. Cetta, G., De Luca, G., Tenni, R., Zanaboni, G., Lenzi, L., and Castellani, A. A. (1983) Biochemical investigations of different forms of osteogenesis imperfecta. Evaluation of 44 cases. *Connect. Tissue Res.* **11,** 103–111
31. Moro, L., Bettica, P., Romanello, M., and Suarez, K. N. (1997) 17 β-estradiol and tamoxifen prevent the overglycosylation of rat trabecular bone collagen induced by ovariectomy. *Eur. J. Clin. Chem. Clin. Biochem.* **35,** 29–33
32. Moro, L., Suarez, K. N., and Romanello, M. (1997) The influence of orchidectomy on collagen glycosylation of trabecular bone in rat. *Eur. J. Clin. Chem. Clin. Biochem.* **35,** 269–273
33. Yang, C. L., Rui, H., Mosler, S., Notbohm, H., Sawaryn, A., and Müller, P. K. (1993) Collagen II from articular cartilage and annulus fibrosus. Structural and functional implication of tissue-specific posttranslational modifications of collagen molecules. *Eur. J. Biochem.* **213,** 1297–1302
34. Amudeswari, S., Liang, J. N., and Chakrabarti, B. (1987) Polar-apolar characteristics and fibrillogenesis of glycosylated collagen. *Coll. Relat. Res.* **7,** 215–223
35. Torre-Blanco, A., Adachi, E., Hojima, Y., Wootton, J. A., Minor, R. R., and Prockop, D. J. (1992) Temperature-induced post-translational overmodification of type I procollagen. Effects of overmodification of the protein on the rate of cleavage by procollagen N-proteinase and on self-assembly of collagen into fibrils. *J. Biol. Chem.* **267,** 2650–2655
36. Notbohm, H., Nokelainen, M., Myllyharju, J., Fietzek, P. P., Müller, P. K., and Kivirikko, K. I. (1999) Recombinant human type II collagens with low and high levels of hydroxylysine and its glycosylated forms show marked differences in fibrillogenesis *in vitro*. *J. Biol. Chem.* **274,** 8988–8992
37. Bätge, B., Winter, C., Notbohm, H., Acil, Y., Brinckmann, J., and Müller, P. K. (1997) Glycosylation of human bone collagen I in relation to lysylhydroxylation and fibril diameter. *J. Biochem.* **122,** 109–115
38. Eyre, D. R., and Glimcher, M. J. (1973) Analysis of a cross-linked peptide from calf bone collagen. Evidence that hydroxylysyl glycoside participates in the crosslink. *Biochem. Biophys. Res. Commun.* **52,** 663–671
39. Hanson, D. A., and Eyre, D. R. (1996) Molecular site specificity of pyridinoline and pyrrole cross-links in type I collagen of human bone. *J. Biol. Chem.* **271,** 26508–26516
40. Robins, S. P. (1983) Cross-linking of collagen. Isolation, structural characterization, and glycosylation of pyridinoline. *Biochem. J.* **215,** 167–173
41. Yamauchi, M., Noyes, C., Kuboki, Y., and Mechanic, G. L. (1982) Collagen structural microheterogeneity and a possible role for glycosylated hydroxylysine in type I collagen. *Proc. Natl. Acad. Sci. U.S.A.* **79,** 7684–7688
42. Yamauchi, M., Katz, E. P., and Mechanic, G. L. (1986) Intermolecular cross-linking and stereospecific molecular packing in type I collagen fibrils of the periodontal ligament. *Biochemistry* **25,** 4907–4913
43. Vogel, W., Gish, G. D., Alves, F., and Pawson, T. (1997) The discoidin domain receptor tyrosine kinases are activated by collagen. *Mol. Cell* **1,** 13–23
44. Jürgensen, H. J., Madsen, D. H., Ingvårsen, S., Melander, M. C., Gardsvoll, H., Patthy, L., Engelholm, L. H., and Behrendt, N. (2011) A novel functional role of collagen glycosylation. Interaction with the endocytic collagen receptor uparap/ENDO180. *J. Biol. Chem.* **286,** 32736–32748
45. Palmieri, D., Valli, M., Viglio, S., Ferrari, N., Ledda, B., Volta, C., and Manduca, P. (2010) Osteoblasts extracellular matrix induces vessel like structures through glycosylated collagen I. *Exp. Cell Res.* **316,** 789–799
46. Livak, K. J., and Schmittgen, T. D. (2001) Analysis of relative gene expression data using real-time quantitative PCR and the $2^{-\Delta\Delta}C_T$ method. *Methods* **25,** 402–408
47. Yamauchi, M., and Shiiba, M. (2008) Lysine hydroxylation and crosslinking of collagen. *Methods Mol. Biol.* **446,** 95–108
48. Yamauchi, M., and Katz, E. P. (1993) The post-translational chemistry and molecular packing of mineralizing tendon collagens. *Connect. Tissue Res.* **29,** 81–98
49. Bailey, A. J., Bazin, S., and Delaunay, A. (1973) Changes in the nature of the collagen during development and resorption of granulatin tissue. *Biochim. Biophys. Acta* **328,** 383–390
50. Eyre, D. (1987) Collagen cross-linking amino acids. in *Methods in Enzymology* (Colowick, S. P., and Kaplan, N. O., eds) pp. 115–139, Academic Press, Inc., Orlando, FL
51. Reynolds, E. S. (1963) The use of lead citrate at high pH as an electron-opaque stain in electron microscopy. *J. Cell Biol.* **17,** 208–212
52. Pornprasertsuk, S., Duarte, W. R., Mochida, Y., and Yamauchi, M. (2005) Overexpression of lysyl hydroxylase-2b leads to defective collagen fibrillogenesis and matrix mineralization. *J. Bone Miner. Res.* **20,** 81–87
53. Parisuthiman, D., Mochida, Y., Duarte, W. R., and Yamauchi, M. (2005) Biglycan modulates osteoblast differentiation and matrix mineralization. *J. Bone Miner Res.* **20,** 1878–1886
54. Mochida, Y., Parisuthiman, D., Pornprasertsuk-Damrongsri, S., Atsawasuwan, P., Sricholpech, M., Boskey, A. L., and Yamauchi, M. (2009) Decorin modulates collagen matrix assembly and mineralization. *Matrix Biol.* **28,** 44–52
55. Gregory, C. A., Gunn, W. G., Peister, A., and Prockop, D. J. (2004) An Alizarin red-based assay of mineralization by adherent cells in culture. Comparison with cetylpyridinium chloride extraction. *Anal. Biochem.* **329,** 77–84

56. Yamauchi, M., Katz, E. P., Otsubo, K., Teraoka, K., and Mechanic, G. L. (1989) Cross-linking and stereospecific structure of collagen in mineralized and nonmineralized skeletal tissues. *Connect. Tissue Res.* **21,** 159–167; discussion 168–159
57. Otsubo, K., Katz, E. P., Mechanic, G. L., and Yamauchi, M. (1992) Cross-linking connectivity in bone collagen fibrils. The COOH-terminal locus of free aldehyde. *Biochemistry* **31,** 396–402
58. Henkel, W., Rauterberg, J., and Stirtz, T. (1976) Isolation of a cross-linked cyanogen-bromide peptide from insoluble rabbit collagen. Tissue differences in hydroxylation and glycosylation of the cross-link. *Eur. J. Biochem.* **69,** 223–231
59. Atsawasuwan, P., Mochida, Y., Parisuthiman, D., and Yamauchi, M. (2005) Expression of lysyl oxidase isoforms in MC3T3-E1 osteoblastic cells. *Biochem. Biophys. Res. Commun.* **327,** 1042–1046
60. Eyre, D. R., and Oguchi, H. (1980) The hydroxypyridinium cross-links of skeletal collagens. Their measurement, properties and a proposed pathway of formation. *Biochem. Biophys. Res. Commun.* **92,** 403–410
61. Yamauchi, M., and Mechanic, G. (1988) Cross-linking of collagen. in *Collagen* (Nimni, M. E., ed) pp. 157–172, CRC Press, Inc., Boca Raton, FL
62. Butler, W. T., and Cunningham, L. W. (1966) Evidence for the linkage of a disaccharide to hydroxylysine in tropocollagen. *J. Biol. Chem.* **241,** 3882–3888
63. Cunningham, L. W., and Ford, J. D. (1968) A comparison of glycopeptides derived from soluble and insoluble collagens. *J. Biol. Chem.* **243,** 2390–2398
64. Morgan, P. H., Jacobs, H. G., Segrest, J. P., and Cunningham, L. W. (1970) A comparative study of glycopeptides derived from selected vertebrate collagens. A possible role of the carbohydrate in fibril formation. *J. Biol. Chem.* **245,** 5042–5048
65. Aguilar, J. H., Jacobs, H. G., Butler, W. T., and Cunningham, L. W. (1973) The distribution of carbohydrate groups in rat skin collagen. *J. Biol. Chem.* **248,** 5106–5113
66. Fietzek, P. P., and Kühn, K. (1976) The primary structure of collagen. *Int. Rev. Connect. Tissue Res.* **7,** 1–60
67. Robins, S. P., and Bailey, A. J. (1975) The chemistry of the collagen cross-links. The mechanism of stabilization of the reducible intermediate cross-links. *Biochem. J.* **149,** 381–385
68. Siegel, R. C., Fu, J. C., and Chang, Y. (1976) Collagen cross-linking. The substrate specificity of lysyl oxidase. *Adv. Exp. Med. Biol.* **74,** 438–446
69. Cronlund, A. L., Smith, B. D., and Kagan, H. M. (1985) Binding of lysyl oxidase to fibrils of type I collagen. *Connect. Tissue Res.* **14,** 109–119
70. Bailey, A. J., Paul, R. G., and Knott, L. (1998) Mechanisms of maturation and ageing of collagen. *Mech. Ageing Dev.* **106,** 1–56
71. Robins, S. P., and Duncan, A. (1983) Cross-linking of collagen. Location of pyridinoline in bovine articular cartilage at two sites of the molecule. *Biochem. J.* **215,** 175–182
72. Eyre, D. R., Dickson, I. R., and Van Ness, K. (1988) Collagen cross-linking in human bone and articular cartilage. Age-related changes in the content of mature hydroxypyridinium residues. *Biochem. J.* **252,** 495–500
73. Robins, S. P., and Bailey, A. J. (1977) Some observations on the ageing in vitro of reprecipitated collagen fibres. *Biochim. Biophys. Acta* **492,** 408–414
74. Gineyts, E., Garnero, P., and Delmas, P. D. (2001) Urinary excretion of glucosyl-galactosyl pyridinoline. A specific biochemical marker of synovium degradation. *Rheumatology* **40,** 315–323
75. Eyre, D. R., Weis, M. A., and Wu, J. J. (2010) Maturation of collagen ketoimine cross-links by an alternative mechanism to pyridinoline formation in cartilage. *J. Biol. Chem.* **285,** 16675–16682
76. Mochida, Y., Duarte, W. R., Tanzawa, H., Paschalis, E. P., and Yamauchi, M. (2003) Decorin modulates matrix mineralization *in vitro*. *Biochem. Biophys. Res. Commun.* **305,** 6–9
77. Kalamajski, S., Aspberg, A., Lindblom, K., Heinegård, D., and Oldberg, A. (2009) Asporin competes with decorin for collagen binding, binds calcium, and promotes osteoblast collagen mineralization. *Biochem. J.* **423,** 53–59
78. Silver, F. H., and Landis, W. J. (2011) Deposition of apatite in mineralizing vertebrate extracellular matrices. A model of possible nucleation sites on type I collagen. *Connect. Tissue Res.* **52,** 242–254
79. Petruska, J. A., and Hodge, A. J. (1964) A subunit model for the tropocollagen macromolecule. *Proc. Natl. Acad. Sci. U.S.A.* **51,** 871–876
80. Sweeney, S. M., Orgel, J. P., Fertala, A., McAuliffe, J. D., Turner, K. R., Di Lullo, G. A., Chen, S., Antipova, O., Perumal, S., Ala-Kokko, L., Forlino, A., Cabral, W. A., Barnes, A. M., Marini, J. C., and San Antonio, J. D. (2008) Candidate cell and matrix interaction domains on the collagen fibril, the predominant protein of vertebrates. *J. Biol. Chem.* **283,** 21187–21197